Extreme Angular Momentum Transport by Gravity Modes in Slowly Pulsating B Stars

Jacqueline Goldstein[1], Rich Townsend[2] & Ellen Zweibel[3]

[1]jgoldstein@astro.wisc.edu; [2]townsend@astro.wisc.edu; [3]zweibel@astro.wisc.edu

We examine angular momentum transport by the single dominant gravity mode observed in three Slowly Pulsating B (SPB) stars: HD24587, HD177863 and HD181558. For each star, we use the MESA code to evolve a structure model matching the measured stellar effective temperature and luminosity. We then apply the GYRE oscillation code to calculate non-adiabatic eigenfrequences and eigenfunctions corresponding to the observed g modes. With mode indices (ℓ,m) and amplitudes fixed to reproduce the observed surface velocity perturbations, there are no free parameters in this process. Based on the g-mode eigenfunctions we evaluate the wave angular momentum luminosity throughout the stars. For all three stars, these luminosities imply that the surface layers could be spun up to critical rotation on timescales as short as months. This tells us that wave transport by opacity-driven g modes can potentially play a significant role in shaping the rotation profiles of SPB stars, and should be incorporated into future stellar evolution calculations.

Introduction

Slowly pulsating B (SPB) stars are intermediate-mass main-sequence stars ($M \sim$ 2-7 $M_\odot$) that exhibit coherent light and spectral variations with characteristic periods of a few days. These variations originate in the stellar-surface velocity and brightness perturbations associated with the global excitation of one or more g-mode oscillations (standing internal gravity waves). The g modes are driven by a standard κ mechanism operating on the radiative opacity peak at $T \sim$ 200,000 K associated with iron-group elements. In this poster we investigate whether the single dominant g mode observed in three SPB stars can modify the stars' rotation over short timescales. The motivation for this study is a series of papers by Ando [1,2,3,4] demonstrating that gravity waves can extract angular momentum from one part of a star and deposit it in another, potentially leading to the development of a strong differential rotation profile. A key aspect of our approach is that we adopt stellar and mode parameters based on empirical measurements, rather than having to rely on ad-hoc assumptions.

Target Selection

The target selection for our study is motivated by three criteria: (i) the star is situated inside the SPB instability strip; (ii) the star's oscillation spectrum is dominated by a single g mode; and (iii) there exist literature values for stellar parameters (effective temperature $T_{\rm eff}$, luminosity L, rotation period $P_{\rm rot}$) and mode parameters (harmonic degree ℓ, azimuthal order m, tangential velocity amplitude $v_{\rm t,max}$). In the study of bright southern SPB stars by [5], three stars meet these criteria: HD24587, HD177863 and HD181558. In all three stars, the oscillation spectrum is dominated by a retrograde dipole g mode: (ℓ,m) = (1,-1). The stellar and oscillation parameters for the stars are summarized in Table 1.

Table 1: Parameters of the SPB stars considered

Star	$T_{\rm eff}$ (K)	log L ($L_\odot$)	$P_{\rm rot}$ (d)	ν (c d^{-1})	$v_{\rm t,max}$ (km s^{-1})
HD 24587	13,860	2.27	2.63	1.1569	4.5
HD 177863	13,380	2.33	2.06	0.84059	47
HD 181558	14,680	2.52	8.55	0.80780	28

Stellar Modeling

We calculate models for the three SPB stars using the MESA stellar evolution code, revision 7385 [6]. We assume solar metallicity following [7], a mixing length parameter α=1.5, and a core overshoot parameter $f_{\rm ov}$=0.3. The mass of each model is automatically adjusted by MESA's *astero* module so that the resulting evolutionary track passes exactly through the desired $T_{\rm eff}$ and L values, as can be seen in Fig. 1.

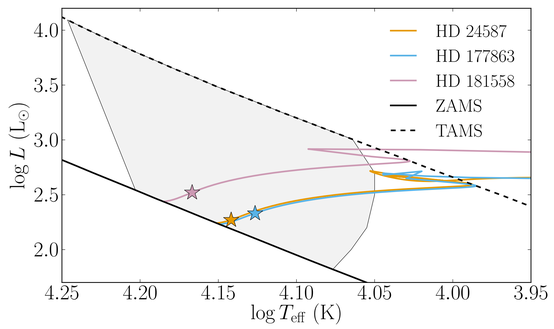

Fig. 1: Herzsprung-Russell diagram showing the positions of the three SPB stars considered, and the corresponding evolutionary tracks calculated by MESA. The grey shading shows the extent of the SPB instability strip for dipole g modes.

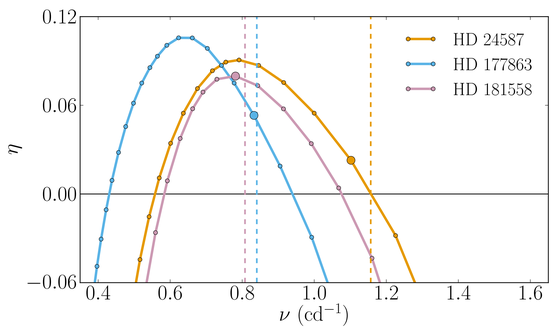

Fig. 2: Normalized growth rate η plotted as a function of the oscillation frequency ν, for dipole g modes of the three model stars. The large circles indicate the modes whose frequencies are closest to the observed frequencies; the latter are shown by the vertical dashed lines (and see also Table 1).

Oscillation Modeling

For each of the three stellar models, we calculate eigenfrequencies and eigenfunctions for (ℓ,m) = (1,-1) g modes using the GYRE oscillation code, version 4.0 [8]. In addition to many other improvements, this release of GYRE incorporates non-adiabatic effects and a non-perturbative treatment of rotation (assumed uniform) using the so-called 'traditional' approximation.

Fig. 2 plots the normalized growth rates η (see [9]) of the g modes, as a function of oscillation frequency ν (as measured in an inertial frame of reference). The figure highlights the specific modes which are closest to the observed frequencies (also shown in the figure, and cf. Table 1). We adopt these 'closest' modes as representative of the dominant oscillation modes seen in the three SPB stars.

Angular Momentum Transport

For the closest modes, we evaluate the wave angular momentum luminosity via the expression

$$L_J = 4\pi r^2 \left\langle r \sin\theta (\rho \overline{v_r v_\varphi}) \right\rangle$$

(cf. [10], their eqn. 10). Here, v_r and v_φ are the radial and azimuthal components of the velocity perturbation, overbars denote the average over azimuth φ, and angle brackets the average over co-latitude θ. To fix the overall amplitude of the velocity perturbations (a free parameter in linear oscillation theory), we match the observed maximum tangential velocities given in Table 1.

Fig. 3 plots the angular momentum luminosities L_J as a function of radius. To interpret these data, note that angular momentum is extracted from regions of the star where $dL_J/dr > 0$, and likewise deposited in regions where $dL_J/dr < 0$. Thus, in all three stars the dominant g mode extracts angular momentum from the inner envelope and deposits it in the outer envelope ($r > 0.9R$).

This angular momentum transport will drive the rotation away from a uniform profile, on a characteristic timescale

$$\tau_{\rm spin} \sim -\frac{8\pi}{3} \rho r^4 \Omega_{\rm crit} \left(\frac{{\rm d}L_J}{{\rm d}r} \right)^{-1}$$

where $\Omega_{\rm crit}$ is the critical angular velocity of the star. Fig. 4 plots $\tau_{\rm spin}$ as a function of radius for each star, clearly revealing how the outer envelope spins up by robbing angular momentum from the interior.

In the surface layers $\tau_{\rm spin}$ becomes very small, indicating that *ceteris paribus* wave transport would spin these layers up to critical rotation on timescales as short as years or even months. Of course, other processes (e.g., shear instabilities) will come into play as soon as the rotation profile becomes non-uniform, and a more detailed calculation is required to determine the ultimate outcome.

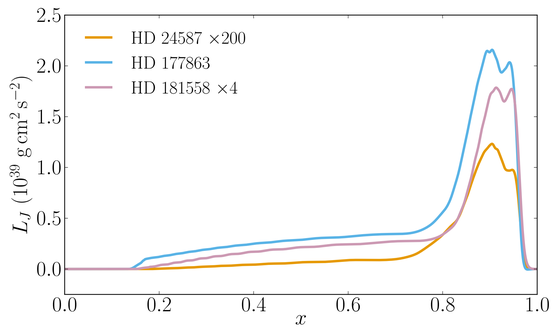

Fig. 3: Angular momentum luminosity L_J plotted as a function of fractional radius x=r/R, for the closest modes in each of the three model stars.

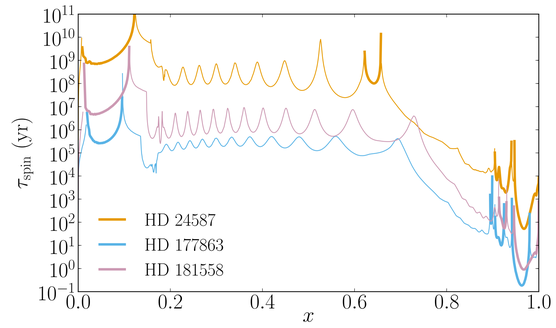

Fig. 4: Spin-up/spin-down timescale $\tau_{\rm spin}$ plotted as a function of fractional radius x=r/R, for the closest modes in each of the three model stars. Thick (thin) lines indicate spin-up (spin-down).

Nevertheless, the results presented here clearly demonstrate that wave transport by κ mechanism-excited g modes can play a significant role in shaping the rotation profiles of SPB stars, and should therefore be incorporated in future stellar evolution calculations.

References: [1] Ando 1981, *MNRAS*, **197**, 1139; [2] Ando 1982, *A&A*, **108**, 7; [3] Ando 1983, *PASJ*, **35**, 343; [4] Ando 1986, *A&A*, **163**, 97; [5] de Cat et al. 2005, *A&A*, **432**, 1013; [6] Paxton et al. 2013, *ApJS*, **208**, 4; [7] Grevesse & Sauval 1998, *SSRv*, **85**, 161; [8] Townsend & Teitler 2013, *MNRAS*, **435**, 3406; [9] Dziembowski et al. 1993, *MNRAS*, **265**, 588; [10] Lee & Saio 1993, *MNRAS*, **261**, 415

Acknowledgements: This research is supported by NASA awards NNX12AC72G and NNX14AB55G, and NSF award ACI-1339600.